Nano World Journal

https://doi.org/10.17756/nwj.2023-s2-040

Research Article

Open Access

Comparative Analysis of Hardening Soil Models and Field Measurements for Deep Excavation: A Numerical Study

Ghizlane Boulaid[1*], Latifa Ouadif[1], Lahcen Bahi[1], Mohamed Ben Ouakkass[1] and Houssine Ejjaaouani[2]

[1]Mohammed V University, Mohammadia School of Engineering, Laboratory of Applied Geophysics, Geotechnics, Engineering Geology and Environment, Rabat 765, Morocco

[2]Public Testing and Research Laboratory, LPEE, Casablanca, Morocco

[*]Correspondence to:
Ghizlane Boulaid
Mohammed V University,
Mohammadia School of Engineering,
Laboratory of Applied Geophysics, Geotechnics, Engineering Geology and Environment,
Rabat 765, Morocco.
E-mail: ghizlane_boulaid@um5.ac.ma

Received: July 25, 2023
Accepted: September 25, 2023
Published: September 28, 2023

Citation: Boulaid G, Ouadif L, Bahi L, Ouakkass MB, Ejjaaouani H. 2023. Comparative Analysis of Hardening Soil Models and Field Measurements for Deep Excavation: A Numerical Study. *NanoWorld J* 9(S2): S232-237.

Copyright: : © 2023 Boulaid et al. This is an Open Access article distributed under the terms of the Creative Commons Attribution 4.0 International License (CCBY) (http://creativecommons.org/licenses/by/4.0/) which permits commercial use, including reproduction, adaptation, and distribution of the article provided the original author and source are credited.

Published by United Scientific Group

Abstract

The increasing urbanization of cities requires the implementation of various subterranean infrastructures, such as tunnels, metro stations, and deep excavations. The construction of retaining structures to support these works can potentially cause structural disturbances to adjacent buildings and structures. Therefore, predicting and controlling ground displacements is crucial. However, estimating these displacements accurately remains a challenging task. This study focuses on a 2D finite element analysis to assess the impact of deep excavations on adjacent structures using two elastoplastic behavior models, the Hardening Soil (HS) model and the Hardening Soil Small (HSS) model. The comparison of the two models and measured values shows that the HSS models provide more accurate predictions of ground surface movements induced by deep excavations. The advanced constitutive model that accounts for small strain characteristics (HSS) outperforms the basic soil constitutive model (HS) in predicting the settlement and displacement of the excavation screen. The use of HSS model can lead to better design and construction practices in deep excavation projects, reducing the risk of damage to surrounding structures and improving the security of the site.

Keywords

Deep excavations, Nailed walls, Hardening soil model, Hardening soil small model, Soil behavior, Field measurements, Displacements, Finite element analysis

Introduction

With the rapid growth of urban areas, the development of large-scale, deep underground excavations has become a topic of interest to researchers. Many studies have been conducted in this area [1-4]. However, the performance of excavation structures can be extremely complex and unpredictable due to uncertainties in soil geology and geomechanics, as well as initial stress conditions. In order to address these uncertainties, Terzaghi and Peck [5] proposed an observational method for soil structures, which is an integrated design-build method. This method has been used in various geotechnical projects [6, 7].

Accurately predicting ground surface settlements and displacements caused by deep excavations using only a basic soil constitutive model can be challenging. On the other hand, adopting an advanced constitutive model of the ground, which considers the small deformation characteristics of the ground, can lead to better predictions of ground surface settlements. However, obtaining input parameters for these advanced soil models can be complex and challenging compared to conventional testing, and they may not always be available. The current study assesses the retaining performance in a 22 meters deep nailed wall of a deep excavation by comparing field measurements with the behavior

models of hardening soil and hardening soil with small strain, particularly in terms of ground surface settlements induced by different stages of deep excavation. Two-dimensional finite element analysis was carried out using the commercial software PLAXIS 2D. The findings of this study could be useful for engineers and researchers using numerical analysis to estimate ground settlements in fractured shales caused by deep excavations.

In the case study, a deep excavation is carried out in Casablanca, Morocco, for the construction of a project that will have five basement levels. In order to carry out the excavation, it is necessary to support the party wall which consists of a 15-storey building on one side and roads on the other three sides. This retaining must be carried out to avoid damage or displacement of the adjacent structures and roads [8, 9]. The method of nail wall retaining will depend on the characteristics of the soil and surrounding environment, and the loading of the excavation (Figure 1).

Figure 1: Retaining braces of the studied façade.

Experimentation

Soil conditions

The excavation site is characterized by a stratigraphy consisting of four soil layers, which include 3 meters of backfill, 2.5 meters of sandstone-limestone, 4.5 meters of highly fractured shale, and 7 to 10 meters of fractured and sound shale. The bedrock of the Casablanca region, which is Paleozoic in age, is folded and contains numerous faults. The cover, consisting of Permo-Triassic, Cretaceous, Miocene, and Plio-Quaternary terrains, is weakly deformed and sub-horizontal. The Cambrian and Ordovician shale is an anisotropic medium and remains a fractured medium with faults extending in all directions. During excavation of the lower layers of the structure, open cracks may develop, and other cracks may form in unpredictable planes. The water table is found at a depth of 3 meters in the sandstone-limestone layer. The provided parameters were obtained from on-site tests, such as pressure meter test, and laboratory tests, such as oedometer and triaxial tests based on core drilling (Figure 2).

Constitutive models

Constitutive models are mathematical descriptions of the behavior of materials, including soils, under various loads and environmental conditions. They are used in engineering and geotechnical fields to predict the response of soil and rocks to various loads, such as those encountered during construction, excavation, and earthquakes. Constitutive models can be based on empirical relationships or on more complex theories, such as mechanics and physics. The accuracy of the predictions made using constitutive models depends on the validity of the model and its parameters, which must be determined from laboratory testing or field observations. Different types of constitutive models exist, including linear and nonlinear models, and they can be used to describe different aspects of soil behavior [10], such as stiffness, strength, and deformation. Constitutive models play a critical role in ensuring the safety and stability of engineering structures and excavations in geotechnical engineering [11-13].

Figure 2: Samples for laboratory testing.

The hardening soil model

The HS model is a nonlinear elasto-plastic soil model designed to simulate the behavior of hardening soils [14, 15]. It incorporates a hyperbolic function to describe the relationship between stress and strain in drained triaxial compression tests. As the model is subjected to deviatoric forces, it displays decreasing stiffness, which is a function of stress, along with irreversible plastic deformation. To capture the behavior of the soil, the model uses three different stress-dependent stiffness parameters, namely E50, which characterizes the stress-strain path resulting from the primary load.

$$E_{50} = E_{50}^{ref}\left(\frac{\sigma_3 \sin\varphi + c\cos\varphi}{p_{ref}\sin\varphi + c\cos\varphi}\right)^m \quad (1)$$

The reference stiffness modulus E_{50}^{ref} corresponds to the reference stress pref, and the actual stiffness depends on the minor principal stress (σ_3), with the magnitude of the stress dependence determined by the power m. The non-linear elastic portion is represented by the stress-dependent unloading and reloading stiffness modulus:

$$E_{ur} = E_{ur}^{ref}\left(\frac{\sigma_3 \sin\varphi + c\cos\varphi}{p_{ref}\sin\varphi + c\cos\varphi}\right)^m \quad (2)$$

The reference stiffness E_{ur}^{ref} at the reference pressure pref is used to model the non-linear stress-strain path of unloading.

This parameter E_{ur} is employed to calculate the non-linear stress-strain path of unloading, which is based on the Hooke elasticity relation for the drained triaxial stress path:

$$\epsilon_1^e = \frac{q}{E_{ur}} \quad (3)$$

The HS model is a constitutive model used to simulate the behavior of soil under various loading conditions. It is a double-hardening plasticity model that includes two types of hardening, shear hardening and cap hardening. The shear hardening yield function controls the behavior of the material during deviatoric stress paths, while the cap-hardening part deals with irreversible compaction in primary compression. The model considers the onset of yielding as soon as the shear strength is mobilized, which leads to an increase in deviatoric plastic strain and a decrease in stiffness. At the point of Mohr-Coulomb failure, failure occurs. The cap yield surface is an ellipse in stress space centered around the origin and is used to compute the plastic volumetric strain, with the current position of the cap determined by the pre-consolidation pressure. The hardening rule determines the evolution of the pre-consolidation pressure with volumetric strain.

$$E_{oed} = E_{oed}^{ref}\left(\frac{c\cos\varphi - \sigma_3'\cos\varphi}{c\cos\varphi - p_{ref}\sin\varphi +}\right)^m \quad (4)$$

In the HS model, the reference odometer stiffness at reference pressure pref is represented by E_{oed}^{ref}. The model requires input of strength parameters: cohesion (c), friction angle (ϕ), and dilatancy angle (ψ), and stiffness parameters such as the secant stiffness at reference pressure in standard drained triaxial test (E_{oed}^{ref}), the tangent stiffness at reference pressure for primary odometer loading (E_{oed}^{ref}), the loading unloading stiffness at reference pressure (E_{ur}^{ref}), the Poisson's ratio for unloading reloading (νur), and a parameter m, which controls the stress-level dependency for all three stiffness parameters.

The hardening soil model with small strain

A modified HSS can explain the behavior of the soil in the small-strain range. As shown in [16-18], the stiffness at these strains is found to be much higher than that determined by conventional tests. The change in stiffness adds two parameters to the HS model to describe the behavior in small strain fields: the initial shear modulus G_0 and the shear strain $\gamma_{0.7}$, where the value of the secant shear modulus is 70% of G_0. The secant shear modulus follows a hyperbolic decrease according to:

$$G_s = \frac{G_0}{1 + 0.385\frac{\gamma}{\gamma_{0.7}}} \quad (5)$$

The collapse stops when the tangential shear modulus Gt reaches Gur. The latter is characterized by the Young's modulus and Poisson's ratio:

$$G_{ur} = \frac{E_{ur}}{2(1+\upsilon_{ur})} \quad (6)$$

Figure 3 illustrates a hardening soil model that considers small deformations, stiffness variation, and shear modulus variation. This model aligns with the findings of previous study [19]. The figure indicates that the soil exhibits a linear elastic behavior and demonstrates a higher stiffness at very low strain rates compared to higher strain rates. These observations emphasize the importance of accounting for strain rate dependency in soil mechanics analysis.

Numerical simulation and field monitoring analysis

Numerical model

Numerical modeling is a widely used technique in the analysis of deep excavation projects in urban areas. This technique involves the creation of a virtual representation of the excavation site and surrounding structures using mathematical equations. By simulating the behavior of the soil and structure under various load conditions, numerical modeling can provide insight into the stability and safety of the excavation and surrounding structures. Deep excavation projects can have a significant impact on the surrounding structures and soils, and numerical modeling can be used to accurately predict the behavior of the soil and structure during the excavation process [20]. This includes changes in soil stiffness, strength, and deformation, as well as the stability of retaining structures such as retaining walls. The PLAXIS software is one example of a tool that can be used for numerical modeling in deep excavation projects.

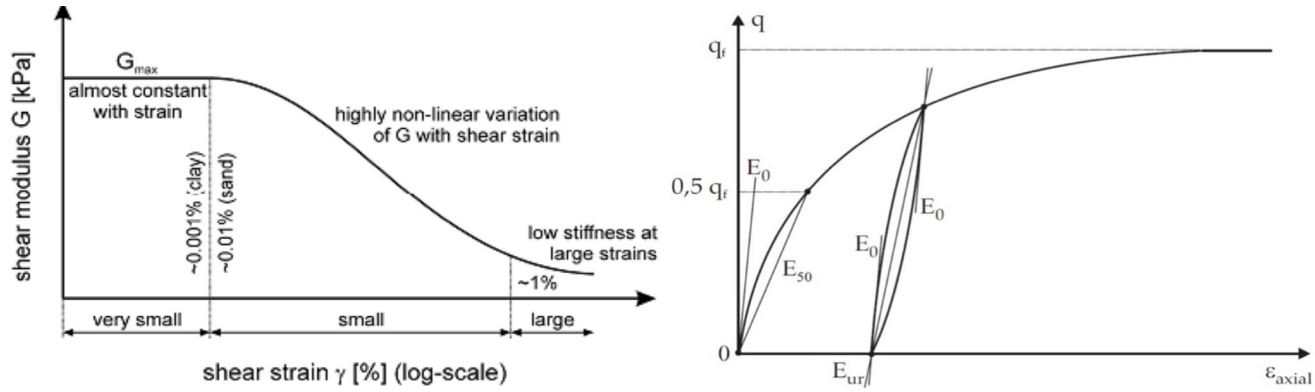

Figure 3: HS model with consideration of small deformations: Variation in stiffness and shear modulus.

Soil modelling

Various constitutive models are available in PLAXIS 2D and can be employed in accordance with the soil input parameters and soil conditions. In this investigation, three material models; Mohr Coulomb, hardening soil, and hardening soil with small deformation stiffness are used. The constitutive models for deep excavations, tunnels, and embankments in PLAXIS 2D that were used in this study for simulation and modeling are all briefly explained below [15, 19].

Soil and structure input parameters

The retaining walls of a 22 meters deep excavation are nailed walls with a nail spacing of 2 meters and a slope of 15°, held in place by a temporary metal strut bed at the head of the wall. Table 1, table 2, and table 3 illustrate the input parameters for the HS and HSS behavior models and the properties of the anchors and excavation walls.

Analysis phases and excavation stages

All analyses are performed using the finite element program PLAXIS 2D. The following computations have been carried out:

- Stage 0: Initialization of geostatic stresses $\sigma'_v = \gamma z$, $\sigma'_h = K_0 \gamma z$ avec $K_0 = 1 - \sin \varphi$;
- Stage 1: Excavation up to 6.50 NGM (under old building slab): with a temporary metal excavation support ;
- Stage 2: Excavation to 4.75 NGM ;
- Stage 3: Activation of the 1st bed of nails at 5.75 + shotcrete up to 4.75 then excavation up to 2.75 NGM ;
- Stage 4: Activation of the 2nd bed of nails at 3.75 + shotcrete to 2.75 then excavation to elevation 0.75 NGM ;
- Stage 5: Activation of the 3rd bed of nails at 1.75 NGM + shotcrete to 0.75 NGM then excavation to -1.25 NGM ;
- Stage 6: Activation of the 4th bed of nails at elevation -0.25 + shotcrete to -1.25 then excavation to elevation -3.25 NGM ;
- Stage 7: Activation of the 5th bed of nails at elevation -2.25 + shotcrete to -3.25 then excavation to elevation -5.25 NGM;
- Stage 8: Activation of the 6th bed of nails at elevation -4.25 + shotcrete to -5.25 then excavation to elevation -7.25 NGM;
- Stage 9: Activation of the 7th bed of nails at elevation -6.25 + shotcrete to -7.25 then excavation to elevation -8.65 NGM; and
- Stage 10: Creation of the 8th bed of nails at elevation -8.25 NGM + shotcrete to -8.65 NGM.

The use of these successive steps allows simulating the excavation process, taking into account the gradual implementa-

Table 1: Geotechnical parameters of the soil layers for the HS model.

Parameters model	Soil layers properties					Unit	Initial estimates
	Backfill	Calcareous sandstone	Fractured shale	Shale	Unfractured shale		
Unsaturated unit weight (γ_d)	20	20	21	21	21	KN/m³	Laboratory testing
Saturated unit weight (γ_s)	20,5	21	21	21	21	KN/m³	Laboratory testing
Effective friction angle (ϕ')	20	35	35	35	35	°	Slope of the rupture line from the Mohr-Coulomb rupture curve
angle of dilation (ψ)	0	5	5	5	5	°	Function of φ'_{peak} and $\varphi'_{critical\ state}$
Effective cohesion (c')	5	80	200	200	200	KN/m²	The ordinate at the origin of the failure line of the Morh Coulomb failure criterion
Poisson's ratio (ν)	0,2	0,2	0,2	0,2	0,2	--	0.2 (default setting)
Axial loading stiffness E_{50}	1600	15,E⁴	1,18,E⁶	1,82,E⁶	1,604,E⁶	kPa	The ordinate in $\log(\sigma'_3/p^{ref})$ - $\log(E_{50})$ curve
Axial unloading stiffness E_{ur}	4800	450,E³	3,53,E⁶	5,48,E⁶	4,81,E⁶	kPa	The ordinate in $\log(\sigma'_3/p^{ref})$ - $\log(E_{ur})$ curve
Oedometer loading stiffness E_{oed}	1600	150,E³	1,18,E⁶	1,83,E⁶	1,60,E⁶	kPa	The ordinate in $\log(\sigma'_1/p^{ref})$ - $\log(E_{oed})$ curve
Power (m)	0,7	0,7	0,7	0,7	0,7	--	Slope of trend-line in $\log(\sigma'_3/p^{ref})$ - $\log(E_{50})$ curve
K_o^{nc}	0,658	0,426	0,426	0,426	0,426	--	1 - sinφ' (default setting)

Table 2: Two additional parameters of soil layers for the HSS model.

Parameters model	Soil layers properties					Unit	Initial estimates
	Backfill	Calcareous sandstone	Fractured shale	Shale	Unfractured shale		
Shear strain magnitude at $0{,}722G_0$ ($\gamma^{0,7}$)	1,E⁻⁴	1,E⁻⁴	1,79E⁻⁵	1,37,E⁻⁵	1,88,E⁻⁵	-	Modulus degradation curve between G/G_0 and $\log_\gamma$
Reference small strain shear modulus G_0^{ref}	2,7,E⁴	2,15,E⁵	3,7,E⁶	5,7,E⁶	5,E⁶	kN/m²	The ordinate in $\log(\sigma'_3/p^{ref})$ $\log(G_0)$ curve

Note: σ_1 is major principle stress (KN/m²); σ_3 is minor principle stress (KN/m²); p_{ref} is reference pressure (100 KN/m²).

Table 3: Anchor and nailed wall parameters.

	Parameters	Symbol	Nails	Shotcrete	Foundation	Unit
Anchor	Material model		Elastic	Elastic	Elastic	
	Normal stiffness	EA	10,00E3			KN
	Spacing	L	2,00			m
Nailed wall	Material model			Elastic	Elastic	
	Normal stiffness	EA1		3,000E^6	20,00E^6	KN/m
		EA2		3,000E^6	20,00E^6	KN/m
	Bending stiffness	EI		5625	1,667E^6	KN m^2/m
	Equivalent thickness	d		0,15	1	m
	Poisson's ratio	υ		0,20	0,20	

tion of the support system through the activation of nail beds and shotcrete. This enables the evaluation of the stability and safety of the construction site at different depths and facilitates the implementation of necessary measures to ensure the robustness of the excavation works. By segmenting the process into stages, a better understanding can be gained of the behavior of the soil and the support systems at each stage of the deep urban excavation process.

Results and Discussion

In this study, we utilized inclinometers and cyclopes as measuring instruments to evaluate the behavior of soil during a deep excavation. These instruments were strategically installed to measure the horizontal displacement of the excavation screen, adjacent structures, and the settlement of the soil behind the nailed walls. The results obtained between September and October 2019 (Figure 4), demonstrated relatively small displacements, ranging from 2 mm to 2.5 mm, which remained below the displacement threshold of 5 mm [21]. These findings indicate that the *in-situ* measurements aligned with the predictions made by the employed models.

Within our study, we conducted a comparison between two distinct finite element soil models: the HS model and the HSS. These models were utilized to simulate the behavior of nail-stabilized soil within fractured shale soil conditions. The comparison results, depicted in figure 5, revealed that the HSS model demonstrated a closer correlation to the actual soil behavior observed *in-situ*. This suggests that the HSS model offers greater accuracy for this particular application involving deep excavation within nail-stabilized fractured shale soil. These outcomes substantiate the effectiveness and reliability of nailing as a stabilization technique for this soil type.

This study underscores the significance of comparing numerical model outcomes with *in-situ* measurements to evaluate the performance of soil behavior models. In our specific case, the HSS model exhibited stronger agreement with the *in-situ* measurements, affirming its capability to accurately predict soil behavior under specific conditions. These findings hold practical implications for the design and planning of deep excavations in soils with similar characteristics.

Conclusion

The study shows that the HSS model can be more accurate and reliable for predicting displacement and settlement in

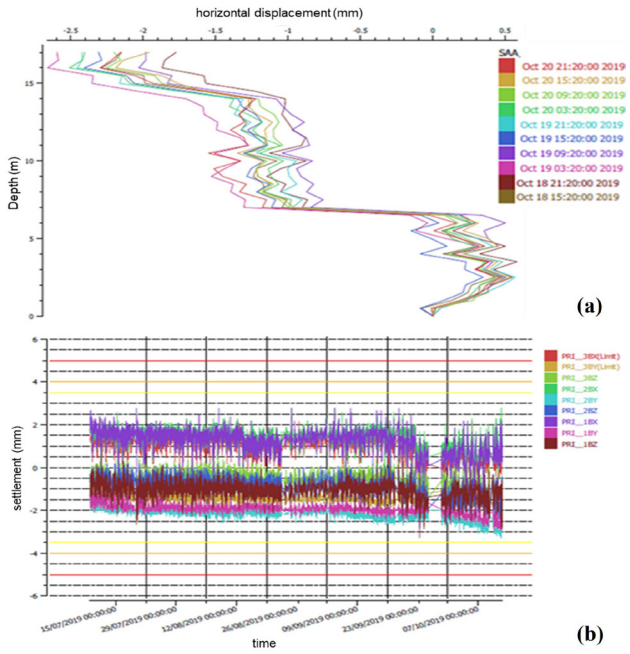

Figure 4: Monitoring lateral movements of nailed wall and adjacent building during excavation: **(a)** Shape accel array measurements and **(b)** Cyclops measurements.

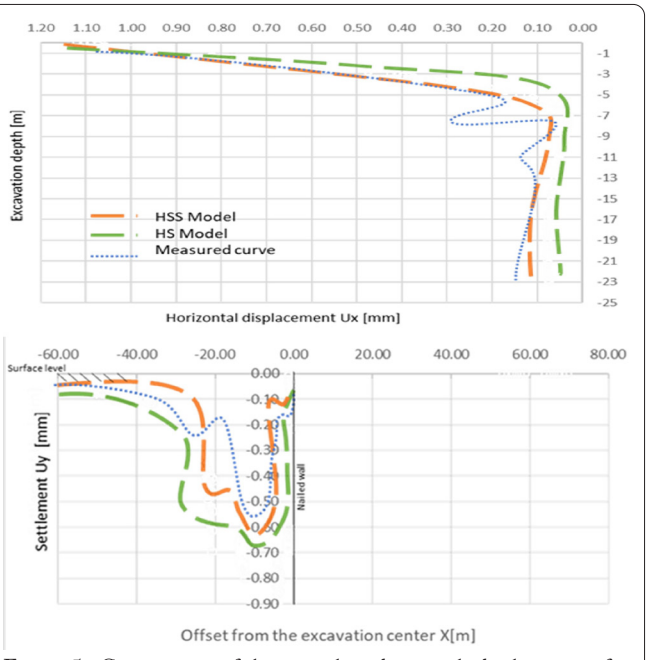

Figure 5: Comparison of horizontal and vertical displacement for monitoring data and finite element results (HS, HSS).

certain scenarios, such as dynamic applications or modelling of unloading-conditioned problems like deep excavations in an urban area. However, the choice of model should ultimately depend on the specific characteristics and conditions of the soil and excavation project being modelled, as well as other factors such as computational efficiency and ease of use. The HSS model is able to account for the stiffness of small deformations and can therefore be used to model the hysteretic behavior of the soil to some extent under cyclic loading conditions. The prediction of the horizontal displacement of the nailed wall based on the drained HSS. A model allows us to confirm the choice of retaining method and also to avoid accidents during excavations.

Acknowledgements

None.

Conflict of Interest

The authors declare that they have no known competing financial interests or personal relationships that could have appeared to influence the work reported in this paper.

References

1. Peck RB. 1969. Deep excavations and tunnelling in soft ground. In Proceeding of 7th ICSMFE.
2. Hsiung BB. 2009. A case study on the behaviour of a deep excavation in sand. *Comput Geotech* 36(4): 665-675. https://doi.org/10.1016/j.compgeo.2008.10.003
3. Khoiri M, Ou CY. 2013. Evaluation of deformation parameter for deep excavation in sand through case histories. *Comput Geotech* 47: 57-67. https://doi.org/10.1016/j.compgeo.2012.06.009
4. Likitlersuang S, Surarak C, Wanatowski D, Oh E, Balasubramaniam A. 2013. Finite element analysis of a deep excavation: a case study from the Bangkok MRT. *Soils Found* 53(5): 756-773. https://doi.org/10.1016/j.sandf.2013.08.013
5. Terzaghi K, Peck RB. 1948. Soil Mechanics. Engineering Practice. John Wiley and Sons, Inc., New York.
6. Spross J, Johansson F. 2017. When is the observational method in geotechnical engineering favourable. *Struct Saf* 66: 17-26. https://doi.org/10.1016/j.strusafe.2017.01.006
7. Fuentes R, Pillai A, Ferreira P. 2018. Lessons learnt from a deep excavation for future application of the observational method. *J Rock Mech Geotech Eng* 10(3): 468-485. https://doi.org/10.1016/j.jrmge.2017.12.004
8. Boulaid G, Bahi L, Ouadif L. 2018. Risk assessment of excavation work of different types of construction projects using AHP. *Int J Civ Eng Technol* 9(12): 861-870.
9. Boulaid G, Latifa O, Bahi L. 2022. Study of the factors affecting the quality and safety of deep excavations in urban areas of Casablanca-Settat province-Morocco. *Int J Adv Sci Eng Inf Technol* 12: 2174. https://doi.org/10.18517/ijaseit.12.6.16264
10. Ti KS, Huat BB, Noorzaei J, Jaafar MS, Sew GS. 2009. A review of basic soil constitutive models for geotechnical application. *Electron J Geotech Eng* 14: 1-18.
11. Hsiung BB, Dao SD. 2014. Evaluation of constitutive soil models for predicting movements caused by a deep excavation in sands. *Electron J Geotech Eng* 19: 17325-17344.
12. Almukashfi A. 2018. Comparison of different constitutive models for deep excavation analysis. Institute of Soil Mechanics, Foundation Engineering and Computational Geotechnics, Graz University of Technology. (Master's Thesis)
13. Nguyen VH, Nikiforova N. 2018. The choice of soil models in the design of deep excavation in soft soils of Viet Nam. In 6th International Scientific Conference on Integration, Partnership and Innovation in Construction Science and Education, Moscow, Russia.
14. Brinkgreve RBJ, Kumarswamy S, Swolfs WM. 2016. PLAXIS 2016. Plaxis bv, Netherlands.
15. Schanz T, Vermeer PA, Bonnier PG. 1999. The Hardening Soil Model: Formulation and Verification. In Brinkgreve RBJ (ed) Beyond 2000 in Computational Geotechnics. A.A. Balkema Publishers, Netherlands, pp 281-296.
16. Jardine RJ, Potts DM, Fourie AB, Burland JB. 1986. Studies of the influence of non-linear stress–strain characteristics in soil–structure interaction. *Geotechnique* 36(3): 377-396. https://doi.org/10.1680/geot.1986.36.3.377
17. Atkinson JH. 1991. Experimental determination of stress-strain-time characteristics in laboratory and-in-situ tests. General report. In proceedings of the 10th European Conference on Soil Mechanics and Foundation Engineering, Florence.
18. Obrzud RF, Truty A. 2018. The Hardening Soil Model - A Practical Guidebook. Zace Services Ltd, Switzerland.
19. Benz T, Schwab R, Vermeer P. 2009. Small-strain stiffness in geotechnical analyses. *Bautechnik* 86(S1): 16-27. https://doi.org/10.1002/bate.200910038
20. Brinkgreve RBJ. 2005. Selection of Soil Models and Parameters for Geotechnical Engineering Application. In Jerry A, Yamamuro PE, Victor NK (eds) Soil Constitutive Models: Evaluation, Selection, and Calibration. American Society of Civil Engineers, pp 69-98.
21. BAEL 91 Rules. 1992. Technical rules for the design of reinforced concrete structures according to the limit states method.